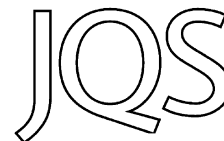# Rapid Communication

West Greenland and global *in situ* ^{14}C production-rate calibrations

JQS

NICOLÁS E. YOUNG,[1]* JOERG M. SCHAEFER,[1] BRENT GOEHRING,[2] NATHANIEL LIFTON,[2]
IRENE SCHIMMELPFENNIG[3] and JASON P. BRINER[4]
[1]Lamont-Doherty Earth Observatory, Columbia University, Palisades, NY 10964, USA
[2]Department of Earth and Atmospheric Sciences, Purdue University, West Lafayette, IN 47907, USA
[3]Aix-Marseille Université, CNRS-IRD, Collège de France, UM34 CEREGE, Aix en Provence, France
[4]Department of Geology, University at Buffalo, Buffalo, NY 14260, USA

ABSTRACT: The *in situ* cosmogenic nuclide ^{14}C is unique compared with other nuclides because of its short half-life, and when combined with longer-lived isotopes (e.g. ^{10}Be), *in situ* ^{14}C can be a powerful tool for deciphering recent and complex surface exposure histories. Like all *in situ* cosmogenic nuclides, quantifying earth surface processes with *in situ* ^{14}C requires a well-constrained *in situ* ^{14}C production rate. We present a production-rate calibration from an independently dated moraine in West Greenland, previously used as an *in situ* ^{10}Be production-rate calibration site. The local *in situ* ^{14}C production rate is 22.8 ± 1.4 atoms g^{-1} a^{-1} (69.28°N, 50.76° W; 350 m asl) and when scaled to sea level/high latitude using time-dependent Lal/Stone scaling (Lm), we calculate a spallation-only *in situ* ^{14}C production rate of 12.0 ± 0.9 atoms g^{-1} a^{-1} and a ^{14}C/^{10}Be production rate ratio of 3.1 ± 0.2. The West Greenland *in situ* ^{14}C production rate is indistinguishable from the New Zealand, Promontory Point and Scottish Highlands *in situ* ^{14}C production rates. When combined, we calculate a global production rate of 12.1 ± 0.5 atoms g^{-1} a^{-1} (Lm). Copyright © 2014 John Wiley & Sons, Ltd.

KEYWORDS: Greenland; *in situ* ^{14}C; production rate; Jakobshavn Isbræ.

Introduction

In situ cosmogenic nuclides ^{10}Be, ^{26}Al, ^{36}Cl, ^{21}Ne and ^{3}He measured in rock surfaces or sediments have revolutionized our ability to place empirical constraints on landscape processes (e.g. Granger *et al.*, 2013). Whereas these isotopes are either stable (^{21}Ne and ^{3}He) or long-lived (e.g. ^{10}Be half-life ~1.39 Ma), *in situ* ^{14}C is a short-lived nuclide with a half-life of 5700 ± 30 years (www.nndc.bnl.gov; Roberts and Southon, 2007) making its use complementary to longer lived isotopes for several geomorphological applications, such as recent and complex exposure–burial histories (e.g. Goehring *et al.*, 2011). In such complex exposure scenarios, *in situ* ^{14}C is relatively insensitive to periods of prior exposure that often result in isotopic inheritance for the longer-lived nuclides, because the portion of the *in situ* ^{14}C inventory accumulated before the last ca. 25 ka will have decayed to undetectable levels. Under conditions of continuous exposure, *in situ* ^{14}C's short half-life results in secular equilibrium (production = decay) after ca. 25–30 ka, and considering uncertainties in both measured concentrations and the secular equilibrium value, the utility of *in situ* ^{14}C for exposure dating is limited to the last ca. 15 ka (Lifton *et al.*, 2001).

There have been relatively few studies using *in situ* ^{14}C measurements (e.g. Yokoyama *et al.*, 2004; Miller *et al.*, 2006; Anderson *et al.*, 2008; Goehring *et al.*, 2011; White *et al.*, 2011; Briner *et al.*, 2014; Hippe *et al.*, 2014). Difficulties isolating small amounts of *in situ* ^{14}C from atmospheric ^{14}C initially limited the application of *in situ* ^{14}C (e.g. Jull *et al.*, 1989). However, a pioneering effort by Lifton *et al.* (2001) focusing exclusively on quartz aliquots (vs. whole rock) significantly improved the reliability of isolating *in situ* ^{14}C and has made its extraction a more reliable technique (Pigati *et al.*, 2010). Nonetheless, *in situ* ^{14}C extraction is still far from routine, given the small number of laboratories currently capable of extracting *in situ* ^{14}C (e.g. ETH Zürich; LDEO, Purdue University) and the remaining challenges in low-background extraction. Studies harnessing *in situ* ^{14}C's potential will undoubtedly increase as more laboratories become able to isolate *in situ* ^{14}C and background ^{14}C concentrations continue to fall (e.g. Hippe *et al.*, 2013; Goehring *et al.*, 2014).

The application of any cosmogenic nuclide requires knowledge of the nuclide-specific production rate. To develop a production-rate calibration, nuclide concentrations must be measured on a surface with a well-constrained exposure history with an independent age, typically derived from radiocarbon dating of organic material. To date, only three *in situ* ^{14}C production-rate calibration experiments exist: Promontory Point (Utah, USA; Lifton *et al.*, 2001; Pigati, 2004; Miller *et al.*, 2006; Dugan *et al.*, 2008), the north-western Scottish Highlands (Dugan *et al.*, 2008) and New Zealand's Southern Alps (Schimmelpfennig *et al.*, 2012). We present an *in situ* ^{14}C production-rate calibration from a site in West Greenland that was previously used for a ^{10}Be calibration (Young *et al.*, 2013a), and then combine this value with existing values to present a 'global' production-rate calibration.

Calibration site: the Marrait moraine at Jakobshavn Isfjord, West Greenland

The Marrait moraine calibration site at Jakobshavn Isfjord (69.15°N, 50.90°W, 350 m asl) is part of the broader Baffin Bay–Arctic ^{10}Be production-rate calibration dataset (Young *et al.*, 2013a). The Baffin Bay ^{10}Be calibration comprises three independent production-rate calibrations: two from the Jakobshavn Isfjord region and one from Baffin Island. Of these three calibrations, the Marrait moraine dataset has the most precise independent age control, and thus we focus on the Marrait moraine to develop our *in situ* ^{14}C production-rate

*Correspondence: N. E. Young, as above.
E-mail: nicolasy@ldeo.columbia.edu

calibration. The full details of this site are provided in Young et al. (2013a), but here we provide a brief overview of the geomorphic setting.

The Jakobshavn Isfjord forefield is dominated by the Fjord Stade moraine system, comprising the older Marrait and younger Tasiussaq moraines (Weidick, 1968; Young et al., 2013b). Following initial deglaciation of the Jakobshavn Isfjord forefield ca. 10 ka, the Marrait moraine was deposited 9175 ± 45 cal a BP (Young et al., 2011). This is the mean age from bracketing ^{14}C ages ($n = 4$; aquatic macrofossils) immediately above and below a dominantly minerogenic sediment unit deposited in the proglacial-threshold Pluto Lake (i.e. Briner et al., 2010) during emplacement of the Marrait moraine. These radiocarbon ages all overlap at 1σ, suggesting that emplacement of the minerogenic unit, and thus the Marrait moraine, was nearly instantaneous (sub-centennial; within dating resolution) and that the radiocarbon ages closely constrain the timing of moraine deposition. Moreover, it is unlikely that hard-water effects influenced our radiocarbon ages because Pluto Lake rests entirely within a crystalline bedrock catchment, and using macrofossils eliminates the potential complications of dating bulk sediments in the Arctic, which often yields radiocarbon ages that are too old (Wolfe et al., 2004). We measured in situ ^{14}C concentrations in quartz from the same five Marrait moraine boulders that were used in the ^{10}Be calibration (Table 1).

In situ ^{14}C measurements and production rate assumptions

In situ ^{14}C extraction was completed in the Lamont-Doherty Earth Observatory (LDEO) extraction line following procedures outlined by Schimmelpfennig et al. (2012) and Goehring et al. (2014). In situ ^{14}C concentrations for five calibration samples were corrected for topographic shielding and sample thickness, but not corrected for potential snow cover. Samples are from open, wind-swept locations, thus minimizing the likelihood of snow cover. Corbett et al. (2011) estimated that nuclide concentrations corrected for snow cover in the Jakobshavn Isfjord region could increase by no more than ~7% for an exposure duration similar to that of the Marrait moraine. This value is almost certainly a significant overestimate because it does not account for sample location and it assumes that all snow remains on the landscape during the winter.

In situ ^{14}C concentrations were blank-corrected using a long-term LDEO blank value of $118.09 \pm 39.28 \times 10^3$ ^{14}C atoms (Table 2a, b), and for each sample, the LDEO blank concentration uncertainty (standard deviation (SD) of 33%) was propagated through in the quadrature (Table 2a). For completeness, we also present uncertainties, including the inter-lab scatter of recent CRONUS-A standard in situ ^{14}C measurements (6.34%; Jull et al., 2014; Table 2a). The arithmetic mean and SD of our corrected in situ ^{14}C concentrations is $126.90 \pm 7.61 \times 10^3$ atoms g^{-1}. The scatter

in the distribution of the calibration in situ ^{14}C concentrations (6%) is greater than the individual 1σ accelerator mass spectrometry (AMS) ^{14}C measurement uncertainties (1%) and greater than the SD of the corresponding ^{10}Be distribution (1%; Table 2a). The standard deviation in our in situ ^{14}C dataset therefore most likely reflects scatter of the LDEO blank values, and reproducibility variations resulting from the complex in situ ^{14}C extraction procedure. The SD of our calibration in situ ^{14}C concentrations is consistent with the SDs of the LDEO CRONUS-A standard measurements (~4.7%; Table 2c) and independent CRONUS-A measurements completed at two other laboratories (~5.0 and 5.7%). Whereas the uncertainty in the ^{10}Be production rate derived from the Marrait calibration samples (~2%; Young et al., 2013a, b) is dictated primarily by the independent age control precision and AMS measurement precision (~2%), our in situ ^{14}C production rate uncertainty is strongly influenced by our intralaboratory measurement repeatability and the scatter of the LDEO long-term ^{14}C blank values.

In situ ^{14}C production occurs until the year of sample collection, 2011 AD for the Marrait moraine calibration samples, whereas traditional radiocarbon ages are reported and calibrated relative to the year 1950 AD. To synchronize these two timescales we added 61 years to the calibrated age of the Marrait moraine and rounded that value (including the uncertainty) to the nearest decade, resulting in an emplacement age for the Marrait moraine of 9240 ± 50 years before 2011. In situ ^{14}C production occurs through spallation and muon capture. Production of in situ ^{14}C by muons (3.8 atoms g^{-1} a^{-1} at sea level/high latitude) is determined separately following Heisinger et al. (2002a, b) and therefore our reported production rates using each scaling scheme are for spallation only (Table 3); our stated local (unscaled) production rate includes spallation and muon capture. We note that the muogenic component of in situ ^{14}C production is not well constrained (Balco et al., 2008) and thus our empirically determined ^{14}C spallogenic production rates and the $^{14}C/^{10}Be$ spallogenic production-rate ratio could change with any future revision of muogenic production rates. Sea-level/high-latitude in situ ^{14}C production rates were determined using the five common scaling schemes [Lal, 1991; Stone, 2000 (St); time-dependent Lal/Stone (Lm); Lifton et al., 2005 (Li); Desilets et al., 2006 (De); Dunai, 2001 (Du)] by selecting the best-fitting ^{14}C production rate through a χ^2 minimization of the misfit between calculated and measured in situ ^{14}C concentrations (Table 3). The χ^2 minimization technique accounts for the uncertainty in our independent age (~50 years), but the total uncertainty is dominated by the distribution and uncertainty in our measured in situ ^{14}C concentrations.

The Marrait moraine calibration site has undergone ~60 m of isostatic uplift since deglaciation. To explore the effects of uplift on our stated production rates, we used a well-constrained regional emergence curve from near our field area and allowed ^{14}C production to vary temporally with increasing elevation along the emergence curve (Long

Table 1. Sample data.

Sample	Latitude (DD)	Longitude (DD)	Elevation (m asl)	Boulder dimensions (L × W × H) (m)	Thickness (cm)	Shielding correction	Thickness correction
11QOO-01	69.2844	−50.7569	350	2 × 1.5 × 1.5	1.5	0.995	0.988
11QOO-02	69.2844	−50.7569	350	1.25 × 1.25 × 1.5	1.5	0.995	0.988
11QOO-03	69.2844	−50.7566	350	2.5 × 1.25 × 1.5	1	0.995	0.992
11QOO-04	69.2844	−50.7562	350	4 × 1.5 × 1.5	1.25	0.995	0.989
11QOO-05	69.2842	−50.7528	350	4 × 4 × 1.75	1	0.996	0.992

For production-rate calculations we assume a rock density of 2.65 g cm^{-3} and a neutron attenuation length of 160 g cm^{-2}.

Table 2a. *In situ* ^{14}C extraction details

Sample	Quartz (g)	V_{CO_2} (cc STP)	V_{dilute} (cc STP)	CAMS no.	F_m measured	^{14}C blank-corrected (10^3 atoms g^{-1})*	^{14}C shielding and thickness-corrected (10^3 atoms g^{-1})*	^{10}Be shielding and thickness-corrected (10^3 atoms g^{-1})†	Local ^{14}C production rate (atoms ^{14}C g^{-1} a^{-1})
11QOO-01	4.9620	0.0917±0.0011	1.505±0.017	161365	0.0167±0.0001	112.94±8.55 (11.51)	114.89±8.70 (11.35)	56.54±1.88 (2.99)	20.6±1.6
11QOO-02	5.1151	0.0304±0.0004	1.402±0.016	162305	0.0206±0.0002	133.07±8.42 (11.92)	135.36±8.56 (12.12)	56.77±1.08 (2.57)	24.3±1.6
11QOO-03	5.0894	0.0235±0.0003	1.367±0.016	161561	0.0203±0.0002	127.00±8.42 (11.65)	128.67±8.53 (11.80)	57.84±1.13 (2.63)	23.1±1.5
11QOO-04	5.1162	0.0503±0.0006	1.370±0.016	162616	0.0199±0.0001	123.40±8.28 (11.39)	125.40±8.42 (11.58)	56.32±1.26 (2.63)	22.5±1.5
11QOO-05	5.1705	0.0536±0.0006	1.312±0.015	162617	0.0215±0.0001	128.61±8.18 (11.55)	130.17±8.28 (11.69)	57.04±1.27 (2.66)	23.4±1.5
					Mean±SD (all measurements)	126.90±7.61 (6.0%)		56.90±0.59 (1.0%)	22.8±1.4 (6.1%)

*The value in parentheses in this column is the uncertainty that includes propagation of the CRONUS-A standard inter-lab scatter (6.3%; Jull *et al.*, 2014).

†The value in parentheses in this column is the uncertainty that includes propagation of the CRONUS-N standard inter-lab scatter (4.1%; Jull *et al.*, 2014).

Sample weight, gas volume after carbon extraction from quartz (V_{CO_2}) and after addition of ^{14}C-free dilution gas (V_{dilute}), cc STP = cubic centimeters at standard temperature and pressure, measured fraction modern (F_m = the ^{14}C/^{13}C ratio of the sample vs. that of a standard, both corrected to δ^{13}C = −25‰ VPDB and to 1950 CE), blank-corrected ^{14}C concentrations with analytical uncertainties, and ^{14}C concentrations corrected for topographic shielding and sample thickness (see Table 1). Also given are the matching ^{10}Be concentrations (Young *et al.*, 2013a), the ^{14}C/^{10}Be concentration ratios and the local time-integrated in situ ^{14}C production rates for each sample.

Table 2b. *In situ* ^{14}C blank and CRONUS-A data.

Sample	Quartz (g)	V_{CO_2} (cc STP)	V_{dilute} (cc STP)	CAMS no.	F_m measured	^{14}C (10^3 atoms)
Blank 2-17-13	n/a	0.02183±0.00025	1.328±0.015	160875	0.0053±0.0001	114.17±12.32
Blank 4-1-13	n/a	0.01933±0.00022	1.363±0.016	161364	0.0047±0.0001	92.61±12.68
Blank 6-13-13	n/a	0.01950±0.00022	1.441±0.017	162306	0.0040±0.0001	69.01±13.28
Blank 8-13-13	5.0150	0.02025±0.00023	1.301±0.016	163860	0.0058±0.0001	129.44±12.37

Blank 8-13-13 is a 'quartz' blank. Quartz is from a recently exposed moraine boulder (<10 years) in the Franz Josef glacier forefield (New Zealand). The measured number of ^{14}C atoms is indistinguishable from the LDEO long-term blank value of 118.09±39.28 × 10^3 ^{14}C atoms. n/a, Not applicable.

Table 2c. LDEO CRONUS-A *in situ* ^{14}C data.

Sample	Quartz (g)	V_{CO_2} (cc STP)	V_{dilute} (cc STP)	CAMS no.	F_m measured	^{14}C (10^3 atoms g^{-1})
CRONUS-A	5.0045	0.06154±0.0007	1.724±0.020	n/a	0.0667±0.0013	642.68±32.80
CRONUS-A-2	4.6503	0.05995±0.0007	1.250±0.014	n/a	0.0754±0.0010	591.54±17.88
CRONUS-A-NM-1	4.9739	0.06141±0.0007	1.381±0.016	151164	0.0807±0.0005	658.78±12.14
CRONUS-A-NM-2	4.9912	0.06710±0.0008	1.437±0.017	151165	0.0803±0.0004	680.81±12.26
CRONUS-A-3-9-11	5.0050	0.07591±0.0009	1.433±0.016	151900	0.0805±0.0004	679.39±12.00
CRONUS-A-3-28-11	5.0211	0.07520±0.0009	1.427±0.016	151901	0.0796±0.0004	665.73±11.85
CRONUS-A-10-28-11	4.9582	0.07891±0.0009	1.515±0.017	163679	0.0743±0.0003	667.26±11.77
					Mean±SD (all measurements)	655.17±30.87 (4.7)

CRONUS-A and CRONUS-A-2 were blank corrected using the LDEO 2009 blank value of 302.09±126.27 × 10^3 ^{14}C atoms (see Goehring *et al.*, 2014). All other samples are blank-corrected using the LDEO long-term (2010 to present) value of 118.09±39.28 × 10^3 ^{14}C atoms. Using this latter blank value results in slightly higher concentrations (<<1%) for A-NM-1, A-NM-2, A-3-9-11 and A-3-28-11 than those reported by Goehring *et al.* (2014), which were corrected using a long-term blank value of 124.67±42.56 × 10^3 ^{14}C atoms.
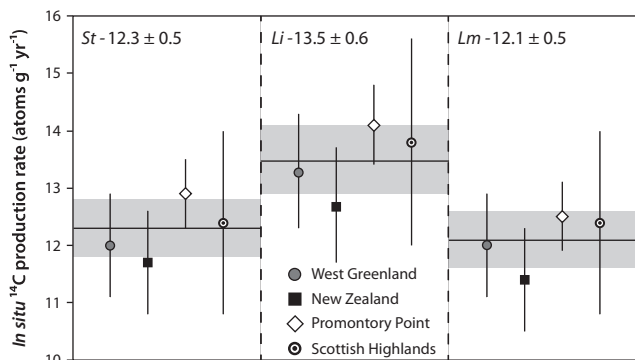
Figure 1. Best-fit *in situ* [14]C production rates (spallation only) using the St, Li and Lm scaling schemes. The horizontal line and gray band is the arithmetic mean and SD of the production-rate values from the four calibration datasets (value at the top of each panel; Table 3).

et al., 2006, 2011; Young *et al.*, 2013a). Applying this correction results in a production rate that is ca. 5% higher than production rates calculated using a constant elevation. This correction, however, would probably result in a maximum-limiting production rate because other processes counteract the effects of isostatic uplift, including changes in air pressure driven by ice sheets and eustatic sea-level change (Staiger *et al.*, 2007; Young *et al.*, 2013a). Lower atmospheric pressure at the ice margin due to katabatic wind effects would lead to an artificially high production rate. For sites exposed since the Last Glacial Maximum, this effect could have been up to ~10% (Staiger *et al.*, 2007), but this should be considered a maximum value here as our calibration site has only been exposed ca. 9200 years. Changes in eustatic sea level near our site would also counteract the effects of isostatic uplift, but the magnitude of this correction is probably minimal (Osmaston, 2005). Adapting the arguments made by Young *et al.* (2013a) and based on the controversial discussion within the surface-exposure dating community regarding the importance of correcting production rates for isostatic rebound (versus countering effects such as sea-level change and air pressure variations), we prefer to use and discuss production rates here that do not include an uplift correction. However, we include rebound-corrected production rates for reference in Table 3.

An *in situ* [14]C production rate from West Greenland

Dividing the average *in situ* [14]C concentration of the five calibration samples ($126.90 \pm 7.61 \times 10^3$ atoms g⁻¹) by the independent age of the Marrait moraine (9240 ± 50 years), results in a time-integrated local *in situ* [14]C production rate at our calibration site (69.28°N, 50.76°W; 350 m asl) of 22.8 ± 1.4 atoms g⁻¹ a⁻¹ (value accounts for the ^{14}C decay constant). Our calculated *in situ* [14]C production rates scaled to sea level/high latitude using the St, Lm, De, Du and Li scaling schemes (for convention) are 12.0 ± 0.9, 12.0 ± 0.9, 12.6 ± 0.9, 12.4 ± 0.9 and 13.3 ± 1.0 atoms g⁻¹ a⁻¹, respectively (Table 3). In addition, the spallation production-rate ratios of ^{14}C/[10]Be for all five scaling schemes are 3.0–3.1 ± 0.2 (Table 3), which agree with the spallation ^{14}C/[10]Be production-rate ratio of 3.0 ± 0.2 determined in the New Zealand calibration samples and with numerically simulated ^{14}C/[10]Be production-rate ratios of 3.1 and 3.2 (Table 3; Masarik and Reedy, 1995; Schimmelpfennig *et al.*, 2012; Argento *et al.*, 2013). We caution that although recent modeling studies support our empirically derived production ratio from a high-latitude and low-altitude location, these

Table 3. Best-fit spallogenic production rates (PR) referenced to sea level/high latitude using the five common scaling schemes.

Scaling	West Greenland in situ [14]C (atoms g⁻¹ a⁻¹)*	West Greenland (atoms [14]C g⁻¹ a⁻¹) uplift*	West Greenland (atoms [10]Be g⁻¹ a⁻¹)	West Greenland ^{14}C/[10]Be PR ratio	New Zealand (atoms [14]C g⁻¹ a⁻¹)*	New Zealand ^{14}C/[10]Be PR ratio	Promontory Point (atoms [14]C g⁻¹ a⁻¹)	Scottish Highlands (atoms [14]C g⁻¹ a⁻¹)	2014 global (atoms [14]C g⁻¹ a⁻¹)†
St	12.0 ± 0.9 (1.1)	12.6 ± 0.9 (1.2)	3.9 ± 0.1	3.1 ± 0.2	11.7 ± 0.9 (1.1)	3.0 ± 0.2	12.9 ± 0.6	12.4 ± 1.6	12.3 ± 0.5 (12.6 ± 0.4)
De	12.6 ± 0.9 (1.2)	13.2 ± 0.9 (1.3)	4.1 ± 0.1	3.1 ± 0.2	11.8 ± 0.9 (1.2)	3.0 ± 0.3	13.1 ± 0.7	13.0 ± 1.7	12.6 ± 0.6 (12.8 ± 0.6)
Du	12.4 ± 0.9 (1.2)	13.0 ± 0.9 (1.2)	4.1 ± 0.1	3.0 ± 0.2	11.9 ± 0.9 (1.2)	3.0 ± 0.3	13.1 ± 0.7	13.1 ± 1.7	12.6 ± 0.6 (12.8 ± 0.5)
Li	13.3 ± 1.0 (1.3)	14.0 ± 1.1 (1.3)	4.4 ± 0.1	3.0 ± 0.2	12.7 ± 1.0 (1.3)	3.0 ± 0.3	14.1 ± 0.7	13.8 ± 1.8	13.5 ± 0.6 (13.7 ± 0.6)
Lm	12.0 ± 0.9‡ (1.1)	12.6 ± 0.9 (1.2)	3.9 ± 0.1	3.1 ± 0.2‡	11.4 ± 0.9 (1.1)	3.0 ± 0.2	12.5 ± 0.6	12.4 ± 1.6	12.1 ± 0.5 (12.2 ± 0.5)

St=Lal (1991), Stone (2000), De = Desilets *et al.* (2006), Du = Dunai (2001), Li = Lifton *et al.* (2005), Lm = time-dependent Lal/Stone. West Greenland refers to the Marrait moraine calibration site (in situ ^{14}C from this study, 10Be from Young *et al.*, 2013a). New Zealand in situ ^{14}C values are from Schimmelpfennig *et al.* (2012); Promontory Point in situ ^{14}C values are from Lifton *et al.* (2001), Pigati (2004), Miller *et al.* (2006) and Dugan *et al.* (2008). The Scottish Highlands in situ ^{14}C dataset is from Dugan *et al.* (2008). The last column shows the arithmetic means and standard deviations of the best-fit values from all four calibration sites. All uncertainties are reported at 1σ.
*Values in parentheses are the uncertainties when including the inter-lab scatter in CRONUS-N standard measurements (Jull *et al.*, 2014).
†Values in parentheses are calculated using the uplift-corrected West Greenland values. Note: the Promontory Point and Scottish Highlands values do not incorporate the CRONUS-N inter-lab scatter.
‡Indicates author's recommended values.

same studies suggest that the production ratio may change as a function of altitude, and perhaps latitude, and thus the production ratio may differ slightly from site to site (Argento *et al.*, 2013; Lifton *et al.*, 2014). The West Greenland production rate of 12.0 ± 0.9 atoms g^{-1} a^{-1} (Lm) is statistically indistinguishable from the New Zealand, Promontory Point and Scottish Highlands production rates of 11.4 ± 0.9, 12.5 ± 0.6 and 12.4 ± 1.6 atoms g^{-1} a^{-1} (Lm), respectively (Table 3).

Combining all four calibration datasets (arithmetic mean $\pm$ SD) results in 'global' ^{14}C production rates of 12.3 ± 0.5 (St), 12.6 ± 0.6 (De), 12.6 ± 0.6 (Du), 13.5 ± 0.6(Li) and 12.1 ± 0.5 (Lm) atoms g^{-1} a^{-1} (Table 3). Note that the use of a 'global' ^{10}Be production rate comprising several individual calibration datasets (Balco *et al.*, 2008) resulted in cases where calculated ^{10}Be ages were incompatible with traditional radiocarbon constraints (e.g. Balco *et al.*, 2009; Briner *et al.*, 2012). However, several recent local *in situ* ^{10}Be production-rate calibrations have resulted in an overall reduction in both the average ^{10}Be production value and its uncertainties (e.g. Balco *et al.*, 2009; Putnam *et al.*, 2010; Young *et al.*, 2013a), such that site-to-site discrepancies evident in the global ^{10}Be dataset are greatly reduced. For locations lacking a local production-rate calibration, our global values for *in situ* ^{14}C spallogenic production are reliable given the stated uncertainties, at least until *in situ* ^{14}C measurement precision improves (e.g. via low and stable blank values) to the point that existing and future calibration datasets are statistically incompatible with the global values reported here.

Conclusions

Our West Greenland *in situ* ^{14}C production rate (12.0 ± 0.9 atoms g^{-1} a^{-1}; Lm) is indistinguishable from the three previously reported production rates from Promontory Point (12.5 ± 0.6; Lm), the Scottish Highlands (12.4 ± 1.6; Lm) and New Zealand (11.4 ± 0.9; Lm). The West Greenland ^{14}C/^{10}Be production-rate ratio of 3.1 ± 0.2 (Lm) is consistent with the empirically derived ^{14}C/^{10}Be production-rate ratio from New Zealand and independently modeled estimates of the production ratio. Combining all four existing *in situ* ^{14}C production rate calibrations, the current *in situ* ^{14}C 'global' production rate is 12.1 ± 0.5 atoms g^{-1} a^{-1} (Lm), a value that is subject to change as more calibration studies become available.

Abbreviations. AMS, accelerator mass spectrometry; LDEO, Lamont-Doherty Earth Observatory

References

Anderson RK, Miller GH, Briner JP, *et al.* 2008. A millennial perspective on Arctic warming from ^{14}C in quartz and plants emerging from beneath ice caps. *Geophysical Research Letters* **35**: L01502.

Argento DC, Reedy RC, Stone JO. 2013. Modeling the earth's cosmic radiation. *Nuclear Instruments and Methods in Physics Research Section B: Beam Interactions with Materials and Atoms* **294**: 464–469.

Balco G, Stone J, Lifton N, *et al.* 2008. A complete and easily accessible means of calculating surface exposure ages or erosion rates from ^{10}Be and ^{26}Al measurements. *Quaternary Geochronology* **3**: 174–195.

Balco G, Briner JP, Finkel RC, *et al.* 2009. Regional beryllium-10 production rate calibration for late-glacial northeastern North America. *Quaternary Geochronology* **4**: 93–107.

Briner JP, Stewart HAM, Young NE, *et al.* 2010. Using proglacial-threshold lakes to constrain fluctuations of the Jakobshavn Isbræ ice margin, western Greenland, during the Holocene. *Quaternary Science Reviews* **29**: 3861–3874.

Briner JP, Young NE, Goehring BM, *et al.* 2012. Constraining Holocene ^{10}Be production rates in Greenland. *Journal of Quaternary Science* **27**: 2–6.

Briner JP, Lifton NA, Miller GH, *et al.* 2014. Using in situ cosmogenic ^{10}Be, ^{14}C, and ^{26}Al to decipher the history of polythermal ice sheets on Baffin Island, Arctic Canada. *Quaternary Geochronology* **19**: 4–13.

Corbett LB, Young NE, Bierman PR, *et al.* 2011. Paired bedrock and boulder ^{10}Be concentrations resulting from early Holocene ice retreat near Jakobshavn Isfjord, western Greenland. *Quaternary Science Reviews* **30**: 1739–1749.

Desilets D, Zreda M, Prabu T. 2006. Extended scaling factors for in situ cosmogenic nuclides: new measurements at low latitude. *Earth and Planetary Science Letters* **246**: 265–276.

Dugan B, Lifton N, Jull AJT. 2008. New production rate estimates for in situ cosmogenic 14C. *Geochimca et Cosmochimica Acta* **72**: A231.

Dunai TJ. 2001. Influence of secular variation of the geomagnetic field on production rates of in situ produced cosmogenic nuclides. *Earth and Planetary Science Letters* **193**: 197–212.

Goehring BM, Schaefer JM, Schluechter C, *et al.* 2011. The Rhône glacier was smaller than today for most of the Holocene. *Geology* **39**: 679–682.

Goehring BM, Schimmelpfennig I, Schaefer JM. 2014. Capabilities of the Lamont–Doherty Earth Observatory in situ ^{14}C extraction laboratory updated. *Quaternary Geochronology* **19**: 194–197.

Granger DE, Lifton NA, Willenbring JA. 2013. A cosmic trip: 25 years of cosmogenic nuclides in geology. *Geological Society of America Bulletin* **125**: 1379–1402.

Heisinger B, Lal D, Jull AJT, *et al.* 2002a. Production of selected cosmogenic radionuclides by muons. *Earth and Planetary Science Letters* **200**: 345–355.

Heisinger B, Lal D, Jull AJT, *et al.* 2002b. Production of selected cosmogenic radionuclides by muons: 2. Capture of negative muons. *Earth and Planetary Science Letters* **200**: 357–369.

Hippe K, Kober F, Wacker L, *et al.* 2013. An update on in situ cosmogenic ^{14}C analysis at ETH Zürich. *Nuclear Instruments and Methods in Physics Research B* **294**: 81–86.

Hippe K, Ivy-Ochs S, Kober F, *et al.* 2014. Chronology of lateglacial ice flow reorganization and deglaciation in the Gotthard Pass area, Central Swiss Alps, based on cosmogenic ^{10}Be and in situ ^{14}C. *Quaternary Geochronology* **19**: 14–26.

Jull AJT, Donahue DJ, Linick TW. 1989. Spallogenic ^{14}C in high-altitude rocks and Antarctic meteorites. *Radiocarbon* **31**: 719–724.

Jull AJT, Scott EM, Bierman P. 2014. In press. The CRONUS-Earth inter-comparison for cosmogenic isotope anlysis. *Quaternary Geochronology*. [doi:10.1016/jquageo.2013.09.003]

Lal D. 1991. Cosmic ray labeling of erosion surfaces: in situ nuclide production rates and erosion models. *Earth and Planetary Science Letters* **104**: 424–439.

Lifton NA, Jull AJT, Quade J. 2001. A new extraction technique and production rate estimate for in situ cosmogenic ^{14}C in quartz. *Geochimica et Cosmochimica Acta* **65**: 1953–1969.

Lifton NA, Bieber JW, Clem JM, *et al.* 2005. Addressing solar modulation and long-term uncertainties in scaling secondary cosmic rays for in situ cosmogenic nuclide applications. *Earth and Planetary Science Letters* **239**: 140–161.

Lifton NA, Sato T, Dunai TJ. 2014. Scaling *in situ* cosmogenic nuclide production rates using analytical approximations to atmospheric

cosmic-ray fluxes. *Earth and Planetary Science Letters* **386**: 149–160.

Long AJ, Roberts DH, Dawson S. 2006 Early Holocene history of the west Greenland Ice Sheet and the GH-8.2 event. *Quaternary Science Reviews* **25**: 904–922.

Long AJ, Woodroffe SA, Roberts DH, *et al.* 2011. Isolation basins, sea-level changes and the Holocene history of the Greenland Ice sheet. *Quaternary Science Reviews* **30**: 3748–3768.

Masarik J, Reedy RC. 1995. Terrestrial cosmogenic-nuclide production systematics calculated from numerical simulations. *Earth and Planetary Science Letters* **136**: 381–395.

Miller GH, Briner JP, Lifton NA, *et al.* 2006. Limited ice-sheet erosion and complex exposure histories derived from in situ cosmogenic ^{10}Be, ^{26}Al, and ^{14}C on Baffin Island, Arctic Canada. *Quaternary Geochronology* **1**: 74–85.

Osmaston HA. 2005. Should Quaternary sea-level changes be used to correct glacier ELAs, vegetation belt altitudes and sea level temperatures for inferring climate changes. *Quaternary Research* **65**: 244–251.

Pigati JS. 2004. *Experimental developments and application of carbon-14 and in situ cosmogenic nuclide dating techniques.* PhD Thesis, University of Arizona.

Pigati JS, Lifton NA, Jull AJT, *et al.* 2010. A simplified in situ cosmogenic ^{14}C extraction system. *Radiocarbon* **52**: 1236–1243.

Putnam A, Schaefer J, Barrell DJA, *et al.* 2010 In situ cosmogenic 10Be production-rate calibration from the Southern Alps. *New Zealand. Quaternary Geochronology* **5**: 392–409.

Roberts ML, Southon JR. 2007. A preliminary determination of the absolute ^{14}C/^{12}C ratio of OX-I. *Radiocarbon* **49**: 441–445.

Schimmelpfennig I, Schaefer JM, Goehring B, *et al.* 2012. Calibration of the *in situ* cosmogenic ^{14}C production rate in New Zealand's Southern Alps. *Journal of Quaternary Science* **27**: 671–674.

Staiger J, Gosse J, Toracinta R, *et al.* 2007. Atmospheric scaling of cosmogenic nuclide production: climate effect. *Journal of Geophysical Research* **112**: B02205.

Stone JO. 2000. Air pressure and cosmogenic isotope production. *Journal of Geophysical Research* **105**: 23,753–23,759.

Weidick A. 1968. Observations on some Holocene glacier fluctuations in West Greenland. *Meddelelser Om Grønland* **165**: 202.

White D, Fülö R-H, Bishop P, *et al.* 2011. Can in-situ cosmogenic ^{14}C be used to assess the influence of clast recycling on exposure dating of ice retreat in Antarctica? *Quaternary Geochronology* **6**: 289–294.

Wolfe AP, Miller GH, Olsen CA, *et al.* 2004. Geochronology of high latitude lake sediments. In *Long-Term Environmental Change in Arctic and Antarctic Lakes*, Pienitz R, Douglass M, Smol J (eds). Springer Verlag: Dordrecht; 19–52.

Yokoyama Y, Caffee MC, Southon JR, *et al.* 2004. Measurements of in situ produced ^{14}C in terrestrial rocks. *Nuclear Instruments and Methods in Physics Research B* **223**: 253–258.

Young NE, Briner JP, Axford Y, *et al.* 2011. Response of a marine-terminating Greenland outlet glacier to abrupt cooling 8200 and 9300 years ago. *Geophysical Research Letters* **38**: L24701.

Young NE, Schaefer JM, Briner JP, *et al.* 2013a. A ^{10}Be production-rate calibration for the Arctic. *Journal of Quaternary Science* **28**: 515–526.

Young NE, Briner JP, Rood DH, *et al.* 2013b. Age of the Fjord Stade moraines in the Disko Bugt region, western Greenland, and the 9.3 and 8.2 ka cooling events. *Quaternary Science Reviews* **60**: 76–90.